Sol–gel synthesis and *in vitro* bioactivity of copper and zinc-doped silicate bioactive glasses and glass-ceramics

2015 Biomed. Mater. 10 025001

(http://iopscience.iop.org/1748-605X/10/2/025001)

Biomedical Materials

PAPER

Sol–gel synthesis and *in vitro* bioactivity of copper and zinc-doped silicate bioactive glasses and glass-ceramics

Julian Bejarano[1], **Pablo Caviedes**[2,3] **and Humberto Palza**[1]

[1] Departamento de Ingeniería Química y Biotecnología, Facultad de Ciencias Físicas y Matemáticas, Universidad de Chile, Santiago, Chile
[2] Centro de Investigación Clínica y Estudios Farmacológicos (CICEF), Facultad de Medicina, Universidad de Chile, Santiago, Chile
[3] Program of Molecular and Clinical Pharmacology, ICBM, Facultad de Medicina, Universidad de Chile, Santiago, Chile

E-mail: jbejarano@ing.uchile.cl

RECEIVED
26 August 2014

REVISED
5 January 2015

ACCEPTED FOR PUBLICATION
29 January 2015

PUBLISHED
11 March 2015

Keywords: sol–gel synthesis, doped bioactive glasses, copper and zinc ions, *in vitro* bioactivity, cytocompatibility

Abstract

Metal doping of bioactive glasses based on ternary $60SiO_2$–$36CaO$–$4P_2O_5$ (58S) and quaternary $60SiO_2$–$25CaO$–$11Na_2O$–$4P_2O_5$ (NaBG) mol% compositions synthesized using a sol–gel process was analyzed. In particular, the effect of incorporating 1, 5 and 10 mol% of CuO and ZnO (replacing equivalent quantities of CaO) on the texture, *in vitro* bioactivity, and cytocompatibility of these materials was evaluated. Our results showed that the addition of metal ions can modulate the textural property of the matrix and its crystal structure. Regarding the bioactivity, after soaking in simulated body fluid (SBF) undoped 58S and NaBG glasses developed an apatite surface layer that was reduced in the doped glasses depending on the type of metal and its concentration with Zn displaying the largest inhibitions. Both the ion release from samples and the ion adsorption from the medium depended on the type of matrix with 58S glasses showing the highest values. Pure NaBG glass was more cytocompatible to osteoblast-like cells (SaOS-2) than pure 58S glass as tested by 3-(4, 5-dimethylthiazol-2-yl)-2, 5-diphenyltetrazolium bromide (MTT) assay. The incorporation of metal ions decreased the cytocompatibility of the glasses depending on their concentration and on the glass matrix doped. Our results show that by changing the glass composition and by adding Cu or Zn, bioactive materials with different textures, bioactivity and cytocompatibility can be synthesized.

1. Introduction

Bioactive glasses and partially crystallized glass-ceramics are recognized as one of the most important biomaterials due to their high biocompatibility and positive biological effects after implantation, forming a direct bond to living bone [1–3]. Sol–gel processing has a number of advantages over traditional melt-quench methods of inorganic biomaterials, such as higher purities and homogeneities, lower processing temperatures, broader ranges of bioactive compositions, higher specific surface areas and rates of apatite layer formation, faster bone bonding, and better degradability and *in vivo* resorption [4, 5]. Moreover, sol–gel allows the easy incorporation of different inorganic ions into the structure of the glasses such as those based on calcium (Ca), phosphorous (P), silicon (Si), copper (Cu), zinc (Zn), boron (B), strontium (Sr), cerium (Ce), vanadium (V), cobalt (Co) and magnesium (Mg) [6–8]. These ions have a physiological role in angiogenesis and in bone metabolism [7, 8], and they can be enzyme cofactors influencing therefore the metabolic signal patterns during tissue formation [9]. Moreover, these ions exhibit various advantages as compared with organic biomolecules (e.g. growth factors) such as low risk of decomposition during the typical manufacturing conditions required for production of inorganic scaffolds and high ability to interact with other ions altering biological functions [6]. In particular, Cu^{+2} and Zn^{+2} ions can be considered as good candidates for the development of doped bioactive glasses due to their osteogenic, angiogenic and anti-bacterial characteristics despite the fact that both ions have been barely studied in these systems [8].

Zn is an important trace element in the body playing a critical role in various functions such as the synthesis of nucleic acids (DNA and RNA). Furthermore, Zn inhibits osteoclast differentiation, plays an important role in the bone formation and shows anti-inflammatory and anti-bacterial effects [7, 8, 10–14]. The incorporation of Zn into bioactive glasses produces higher chemical stability and densification of glasses matrices [15]. However, the effect of Zn on the *in vitro* bioactivity is not

consistent as some studies found that this ion does not affect this property [16], whereas other studies showed an inhibitory effect [17–19]. Therefore, more research about the bioactivity of Zn-doped glasses is necessary.

Cu otherwise is essential for human life forming part in enzymes of great importance for the normal functioning of the body [20]. It is an angiogenic agent because of increases the expression of pro-angiogenic and growth factors (VEGFs), enhances the *in vivo* angiogenesis, and stimulates the human endothelial cell proliferation [12, 21–23]. Cu has been incorporated in various materials used in biomedical applications showing anti-bacterial and angiogenic properties, and a role in collagen deposition, cellular activity and proliferation of osteoblasts [11, 24–27]. The *in vitro* bioactivity of Cu-doped glasses was dependant on the concentration of metal ion incorporated which inhibited the formation of apatite at higher concentrations [24, 25]. Similar to what was observed in Zn-doped glasses, the incorporation of Cu also increased the chemical durability and mechanical strength of the glasses [25] and promoted an anti-inflammatory prophylactic effect [11]. Recently, our research group prepared Cu-doped glasses by sol–gel showing anti-bacterial properties against *E. coli* and *S. mutans* bacteria [26]. These results suggest that Cu has interesting multifunctional properties for use in regenerative medicine.

Despite the above mentioned, more studies relating the microstructure and the composition of Cu and Zn-doped bioactive glasses with their ion release during dissolution and biological performance, are necessary. This is even more relevant as there is a lack of studies comparing the effect of Zn^{+2} and Cu^{+2} ions in sol–gel based bioactive glasses. The objective of this study is to synthesize ternary and quaternary sol–gel bioactive glasses doped with different concentrations of Zn and Cu. A comparative study was conducted on the effect of these ions on the microstructure of the glasses and the ability to form an apatite surface layer after soaking in simulated body fluid (SBF). The release of these metal ions from the bioactive glasses and its cytocompatibility with osteoblast-like cells was also evaluated.

2. Materials and methods

2.1. Sol–gel synthesis

The compositions and codes of the different samples are displayed in table 1. The glasses were synthetized by sol–gel process using as precursors tetraethyl orthosilicate (TEOS, Aldrich, 98%), triethylphosphate (TEP, Aldrich, 99.8%), sodium nitrate (Riedel-de Häen, 99.5%) and calcium nitrate tetrahydrate (Merck, 99%) for the undoped glasses. For the metal-doped glasses either copper nitrate trihydrate (Merck, 99.5%) or zinc nitrate tetrahydrate (Merck, 98.5%) were used. The hydrolysis of TEOS and TEP was catalyzed with a 0.1 M solution of HNO_3 using a molar ratio $(HNO_3+H_2O)/(TEOS+TEP)$ of 8. The sol was obtained from the hydrolysis of TEOS, adding the other reagents sequentially to obtain the specific composition displayed in table 1. with 45 min intervals under constant stirring. When the last reagent was added, the mixture was stirred for 60 min. The resultant sols were poured into high density polyethylene vessels and stored for 3 d at room temperature. After this period, the gels were dried at 60 °C and 130 °C for 3 and 2 d, respectively. The dried gels were crushed in an analytic mill and placed in ceramic crucibles for heat treatment in an electric furnace under oxidizing atmosphere (air) at 700 °C. Finally, the resulting powder was manually milled in an agate mortar, and then it was sieved through a 200 mesh sieve (<75 μm), selected and characterized.

Table 1. Chemical composition of the glasses synthetized.

Glass code	Glass composition (mol%)					
Ternary glasses	SiO_2	CaO	Na_2O	P_2O_5	CuO	ZnO
58S	60	36	*	4	*	*
1Cu–58S	60	35	*	4	1	*
5Cu–58S	60	31	*	4	5	*
10Cu–58S	60	26	*	4	10	*
1Zn–58S	60	35	*	4	*	1
5Zn–58S	60	31	*	4	*	5
10Zn–58S	60	26	*	4	*	10
Quaternary glasses						
NaBG	60	25	11	4	*	*
1Cu–NaBG	60	24	11	4	1	*
5Cu–NaBG	60	20	11	4	5	*
10Cu–NaBG	60	15	11	4	10	*
1Zn–NaBG	60	24	11	4	*	1
5Zn–NaBG	60	20	11	4	*	5
10Zn–NaBG	60	15	11	4	*	10
1Cu1Zn–NaBG	60	23	11	4	1	1

* Glass does not contain this oxide in its composition.

2.2. Glass particles characterization

Mean particle size of sol–gel powders was determined by laser diffraction analysis, using a Mastersizer 2000 (Malvern Instruments, USA) granulometer. The specific surface area and pore volume and size of the particles were measured by nitrogen adsorption in a Micromeritics ASAP 2010 sorptometer at −196 °C using the Brunauer, Emmett and Teller and Barrett, Joyner, and Halenda methods. Samples were previously pretreated at 200 °C in vacuum for 2 h. The structure and the phases present in the glasses were analyzed by a Bruker model D8 Advance x-ray diffractometer (XRD) using a lineal detector LynxEye, CuKα radiation $\lambda = 1.5418$ Å, nickel filter system and variable slit. The diffractometer was operated at 40 kV and 30 mA at a 2θ range of 20–50°, using coupled scanning with a step size of 0.02° s^{-1}.

2.3. In vitro bioactivity evaluation and dissolution in SBF

To evaluate the bioactivity of the synthesized glasses, *in vitro* tests were performed according to the method

described by Kokubo and Takadama [28] using a solution known as SBF with a sample mass to volume of SBF ratio of 0.01 g ml^{-1}. During the tests, the samples were in contact with the SBF solution for periods of 1, 7 and 14 d at 37 °C. Then, the samples were removed from their bottles and washed with acetone. Finally, the dried powders were characterized using XRD, Fourier transform infrared attenuated total reflectance spectroscopy (FTIR-ATR, Agilent Technologies model Cary 630) and scanning electron microscopy (SEM) with x-ray microanalysis (SEM/EDS, FEI model Quanta 250) to evaluate the formation of a calcium phosphate (CaP) layer on their surface. For SEM analysis samples were coated with a gold layer and then analyzed. Concentrations of Ca^{+2} and PO_4^{-3} ions in the SBF after glass particle dissolution were analyzed for each testing time to relate them with the bioactivity evolution. Measurements of Ca^{+2} ions were performed using an atomic absorption spectrometry (AAS, Perkin Elmer 1100 B spectrophotometer). Total PO_4^{-3} ions were measured by colorimetry using a vanadate–molybdate solution and the absorbance measured at 400 nm. The result were expressed as mean ± standard deviation (SD) for $n = 3$.

2.4. *Cu^{+2} and Zn^{+2} ion release and pH changes*

Cu^{+2} and Zn^{+2} ion release and pH changes were evaluated by immersing bioactive glasses in a cell culture media Dulbecco's modified Eagle's medium (DMEM/F12, Gibco® by life technologies) to relate it with the glass cytocompatibility. Glass powders were added to the culture medium at a concentration of 0.01 g ml^{-1}. The samples were placed in an incubator shaker (Zhigheng, model 100B) at 200 rpm and 37 °C during 1, 3, 7 and 14 d. The concentrations of ions within the culture medium were measured using AAS. pH changes for each testing time were measured with a pH meter (Jenco Electronics Ltda, model 1671). The results were expressed as mean ± standard deviation (SD) for $n = 3$.

2.5. In vitro cytocompatibility

Cytotoxicity of the bioactive glasses was evaluated by 3-(4,5-dimethylthiazole-2-yl)-2,5-diphenyltetrazolium bromide (MTT) assay (USB Corporation, USA) as per standard protocol to assess cell viability [29, 30]. Briefly, the method is based on the ability of living cells to reduce tetrazolium salts into formazan derivatives. Human osteosarcoma cell line (SaOS-2) was seeded in DMEM/F12 supplemented with 10% fetal bovine serum (FBS), gentamicin (40 mg l^{-1}) and 1 μl ketokonazol (5 mg ml^{-1} of phosphate buffer solution (PBS)) ml^{-1} culture media, at a density of 5×10^3 cells per well (150 μl of culture media). The bioactive glasses samples, sterilized by autoclave and UV light during 30 min, were immersed per well in a material mass to culture media volume ratio of 0.01 g ml^{-1}. After 24 h of culture in an incubator at 37 °C and humidified atmosphere (5% CO_2 in 95% air), the previous culture media was removed and each well washed with a PBS. 100 μl of media with MTT (80 μl of MTT (5 mg ml^{-1}) per ml of DMEM/F12 without FBS) was added to each well and incubated during 3 h. After incubation the media containing MTT was removed from the 96-well plate and 200 μl of isopropyl alcohol was added per well to dissolve the formazan crystals. The optical density of the solution was measured at 540 nm by a microplate reader (Titerket® Multiskan® MCC/340, MKII) and cell viability calculated. The MTT assay per each bioactive glass was performed with $n = 6$ and three independent experiments. The cells cultured with DMEM/F12 media acted as control.

Table 2. Textural characterization of the glass particles synthesized.

Glass code	Particle properties					
Ternary system	A_s (μm)			S_a ($m^2 g^{-1}$)	V_p ($cm^3 g^{-1}$)	Mean Dia. (nm)
	d_{10}	d_{50}	d_{90}			
58S	7.0	37.5	80.3	82	0.201	10
1Cu–58S	3.5	28.1	69.3	130	0.476	14
5Cu–58S	3.9	30.9	72.8	145	0.464	13
10Cu–58S	5.6	36.6	82.0	105	0.266	10
1Zn–58S	4.9	37.8	77.2	123	0.445	14
5Zn–58S	5.4	37.1	79.6	124	0.355	11
10Zn–58S	5.6	38.9	81.6	70	0.145	8
Quaternary system						
NaBG	7.8	32.6	64.4	15	0.035	13
1Cu–NaBG	2.4	33.7	65.3	2	0.003	6
5Cu–NaBG	2.6	35.8	67.6	2	0.005	18
10Cu–NaBG	5.4	31.3	69.6	2	0.008	12
1Zn–NaBG	4.5	34.2	70.8	3	0.009	10
5Zn–NaBG	4.8	36.0	82.7	3	0.006	11
10Zn–NaBG	4.0	31.1	73.8	2	0.007	10

A_s: average particle size, S_a: specific surface area, V_p: pore volume, Dia.: pore diameter.

3. Results and discussions

3.1. Textural and microstructural characterization of glass particles

The properties of the glass particles synthesized by sol–gel are shown in table 2. The average particle sizes d_{50} were similar for all the samples with values between 30 to 40 μm and therefore during our analysis will not be a variable to discuss. The textural properties and microstructure of the undoped glasses depended on their compositions. 58S glass presented higher both specific surface area (82 $m^2 g^{-1}$) and pore volume (0.201 $cm^3 g^{-1}$) than NaBG glass (15 $m^2 g^{-1}$ and 0.035 $cm^3 g^{-1}$, respectively) although the pore sizes were similar for both glasses. These differences are related with the presence of Na_2O in the quaternary system decreasing the melting point and generating therefore a sintering processes between primary particles during the treatment at 700 °C [31, 32]. X-ray diffractograms (XRD) displayed in figure 1 show that both 58S and

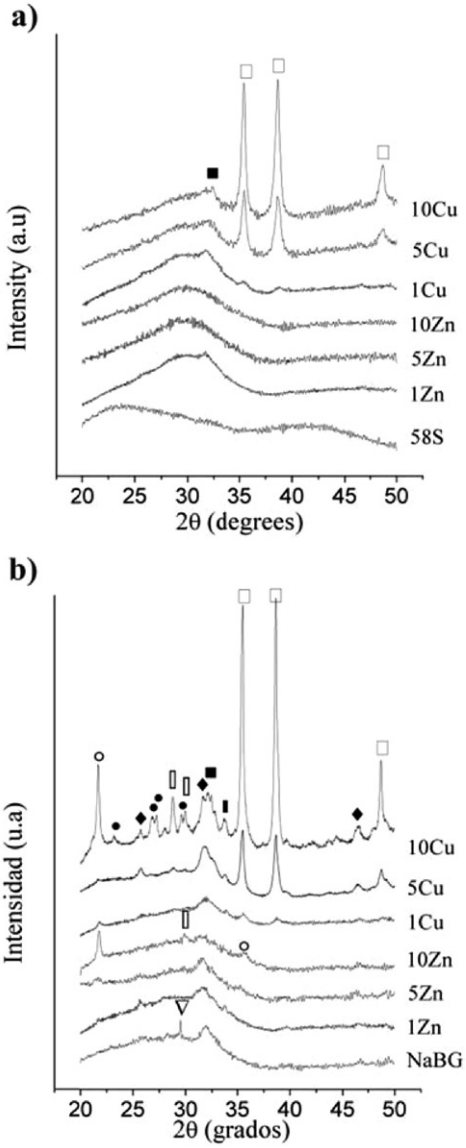

Figure 1. X-ray diffractograms of undoped and Cu and Zn doped 58S (*a*) and NaBG (*b*) glasses. Crystal phases with their JCPDS codes are labeled as follow: (□) CuO (01-089-5899), (■) Ca_2SiO_4 (00-029-0369), (♦)$Na_2Ca_4(PO_4)_2SiO_4$ (32-1053), (●) $Na_2Ca_3Si_6O_{16}$ (00-023-0671), (▮) Na_2CaSiO_4 (01-073-1726), (▯) $CaSiO_3$ (01-072-2284), (∇) $CaCO_3$ (01-085-1108), (○) Cristobalite (SiO_2, 01-082-0512).

NaBG glasses presented mainly amorphous structure. However, the NaBG glass displayed a broad peak around $2\theta = 32°$ likely corresponding to a partial crystallization of an apatite-like phosphate (silicorhenanite, $Na_2Ca_4(PO_4)_2SiO_4$) or calcium silicate (Ca_2SiO_4) (figure 1(*b*)). This partial crystallization has been observed in other quaternary glasses after calcination process [32, 33]. The presence of calcite ($CaCO_3$) in NaBG was further observed with its main peak at $2\theta = 29.5°$.

The effect of Cu and Zn on the textural properties and microstructure of the doped glass matrices depended on their compositions. The incorporation of Cu and Zn increased the surface area and the pore volume of 58S as reported previously [34, 35] whereas an opposite effect was observed in NaBG-based glasses in agreement with previous studies about the incorporation of Zn [17, 36] and Cu [25, 37] in silicate glasses [17]. XRD from figure 1 showed that the incorporation of Cu generated copper oxide (CuO) in both glasses (58S and NaBG) as peaks at $2\theta = 35.6°$ and 38.8° were developed. The presence of CuO crystals in these systems depends on both the conditions used during the sol–gel process and the amount of copper added, and it appears together with homogeneous dissolved Cu ions, as reported previously [26, 37–39]. The incorporation of Cu in NaBG promoted the formation of an apatite-like phase together with Ca_2SiO_4 crystals and at the highest amount of Cu (10Cu–NaBG) the formation of cristobalite (SiO_2), coesite (SiO_2) and calcium silicates ($Na_2Ca_3Si_6O_{16}$, Na_2CaSiO_4, $CaSiO_3$, Ca_2SiO_4) was favored, meaning a glass–ceramic material. This formation of the apatite-like phase (silicorhenanite), before immersion in SBF (as-prepared), and the other crystalline phases could be explained by the formation and separation of crystalline phases induced by Coulombic repulsions of the Cu^{+2} ions with the other modifier ions (Ca^{+2} and Na^{+}) as has been reported previously for silicate glasses [25, 40]. This Coulombic repulsions are due to the high ionic potential of the Cu^{+2} ions and the octahedral coordination (CN = 6), which make to the Cu^{+2} ions a true network modifiers and this further produce immiscibility and phase separation [40, 41]. The incorporation of Zn in 58S did not generate any new crystalline phases while in NaBG the initial crystallization of apatite and Ca_2SiO_4 was inhibited. These results show that the final microstructure of these glasses depends on the metal used and the composition of the glass matrix.

3.2. Apatite-forming ability and dissolution after soaking in SBF

58S and NaBG glasses presented *in vitro* bioactivity after immersion in SBF as confirmed by XRD and FTIR results (figure 2) showing apatite layer formation after soaking times of 1, 7 and 14 d. 58S glass (figures 2(*a*) and (*b*)) developed a CaP phase formed by crystalline apatite (HA) showing peaks at $2\theta = 25.9°$ and 32° (figure 2(*a*)) after the first day of soaking [26]. As time elapsed, the HA layer on the surface of the sample increased as concluded by both the larger intensity of its original peaks and the new characteristic peaks at $2\theta = 46.7°$ and 49.5° [26]. The bioactivity was also evidenced by FTIR spectra (figure 2(*b*)) with the appearance from the first day of soaking, of the bands at 562 and 602 cm^{-1} associated with the anti-symmetric bending of the P–O bond of the apatite crystal [42]. The band around 1060 cm^{-1} corresponding to the anti-symmetric stretching of the P–O bond was also observed in figure 2(*b*) [25, 38, 39]. The diffractogram of NaBG displayed in figure 2(*c*) also showed the appearance of the characteristic peaks of HA after the first day of soaking in SBF. However, an improved crystallization of HA was observed in this sample as another characteristic peak appeared at $2\theta = 39.7°$ increasing its intensity as time elapsed. At 14 d of soaking, the main peak of $CaCO_3$ at $2\theta = 29.5°$ increased its intensity while new $CaCO_3$ peaks were developed

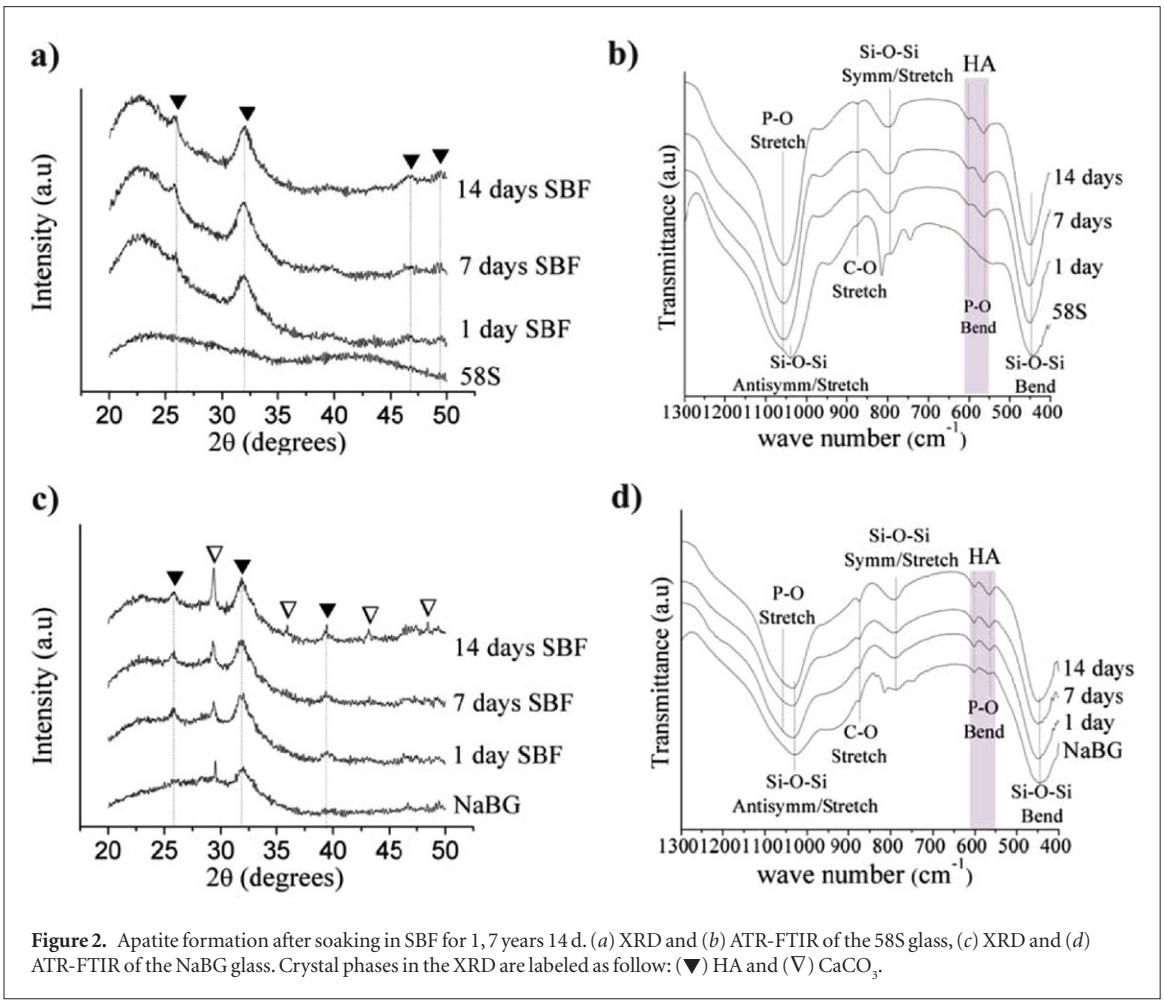

Figure 2. Apatite formation after soaking in SBF for 1, 7 years 14 d. (*a*) XRD and (*b*) ATR-FTIR of the 58S glass, (*c*) XRD and (*d*) ATR-FTIR of the NaBG glass. Crystal phases in the XRD are labeled as follow: (▼) HA and (∇) $CaCO_3$.

showing adsorption of carbonates groups from SBF. The bioactivity of the NaBG was also followed by FTIR (figure 2(*d*)) confirming XRD results due to the appearance of the doublet at 562 and 602 cm^{-1}. The formation of a HA layer on the surface of 58S and NaBG glasses after soaking in SBF was further corroborated by SEM and energy dispersive x-ray spectroscopy (EDS). Figures 3(*a*) and (*b*) shows the formation of spherical particles or granules on the surface of the glasses that is the characteristic morphology of apatite crystals formed by biomineralization [43–45]. NaBG glass presented both more and larger granules on the surface than 58S glass showing differences in the apatite formation and its morphology. The higher porosity of 58S permitting the formation of smaller apatite crystals could explain this behavior. Values coming from EDS between 1.5 and 1.8 for the Ca/P atomic ratios of these surface layers (data not shown) were around the stoichiometric ratio reported for HA (1.67) [46]. Similar ratios have been reported for apatites having bioactivity and ability to bind to bone [38, 47, 48]. These results showed therefore that undoped 58S and NaBG glasses have high *in vitro* bioactivity and the potential ability of binding to bone tissue.

Bioactive glasses during soaking in SBF suffer dissolution processes releasing different ions [2, 9]. The apatite layer formed on the surface of silicate-based glasses is consequence of the diffusion-out of Ca^{+2} from the glass surface and subsequent migration of Ca^{+2} and PO_4^{-3} ions on an amorphous silica layer formed in the glass surface, according to the reactions proposed by Hench [2]. Figure 4 shows the concentration of Ca^{+2} and PO_4^{-3} ions in SBF after soaking 58S and NaBG glasses for 1, 7 and 14 d. The release of Ca^{+2} ions from 58S-derived glasses was larger than those from NaBG-derived glasses (figures 4(*a*) and (*b*)) because of their higher surface areas and pore volumes facilitating dissolution processes (table 1). This effect was also concluded previously by observing that an increased specific surface area promotes the glass dissolution and the ion release of bioactive glasses [42, 49]. The Ca_2SiO_4 and CaP crystals formed during the synthesis of NaBG stabilizing a part of Ca^{+2} ions in the glass should be further taken into account. Regarding the dynamic of phosphorous ions (PO_4^{-3}), its initial concentration in SBF was reduced as time elapsed showing an adsorption process (figures 4(*c*) and (*d*)). Undoped 58S and NaBG glasses adsorbed greater amount of PO_4^{-3} from SBF during the first day with six times higher adsorption in 58S sample due to its larger surface area.

After soaking the particles in SBF, a relevant effect of the incorporation of Cu and Zn on the apatite formation was observed depending on the metal ion and matrix composition, as displayed in figure 5. The results of both XRD after immersion in SBF and the ion release showed that the incorporation of Cu and Zn affects the

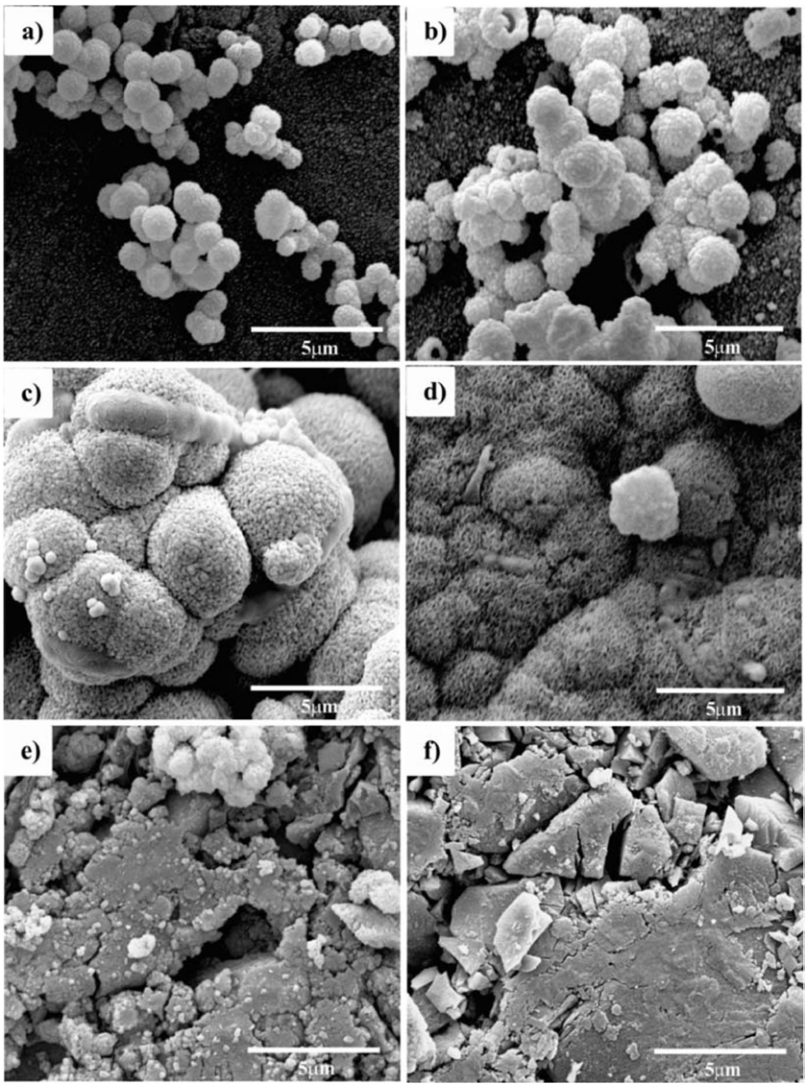

Figure 3. SEM images of undoped and Cu and Zn doped glasses after 7 d in SBF. (*a*) 58S, (*b*) NaBG, (*c*) 1Cu–58S, (*d*) 1Cu–NaBG, (*e*) 1Zn–58S and (*f*) 1Zn–NaBG.

durability or chemical stability of the doped glasses. This conclusion is based on the formation of new crystal phases together with the generation of a glass structure with higher network connectivity, both characteristics having as consequence a lower dissolution process and the inhibition of the conversion from amorphous CaP to HA by the lower diffusion of Ca^{+2} and PO_4^{-3} ions [18, 25, 34, 50, 51]. Although the diffractograms were performed in samples soaked at different times up to 14 d, for clarity the figure 5 displays results only for tests lasting 7 d as at shorter and longer times the samples displayed the same tendency. The presence of Cu in the 58S glass decreased the ability to form surface crystalline apatites for all percentages of metal incorporated (figure 5(*a*)) as concluded by the lower intensity of the HA peaks after immersion in SBF. The competition between Cu^{+2} and Ca^{+2} ions in solution for the precipitation of phosphate species can explain the lower bioactivity of the doped glasses [25, 35]. For the incorporation of Cu in the NaBG glass (figure 5(*b*)) otherwise did not significantly affected the formation of HA. Calcium silicates ($Na_2Ca_3Si_6O_{16}$, Na_2CaSiO_4, $CaSiO_3$, Ca_2SiO_4) from 10Cu–NaBG suffered dissolution during the soaking in SBF decreasing their characteristics peaks. Cristobalite and CuO crystals were more stable in SBF without appreciable dissolution. SEM images from 1Cu–58S and 1Cu–NaBG samples at 7 d of immersion in SBF (figures 3(*b*) and 3(*c*)) confirmed the formation of crystal apatite with the typical topography in accordance with other studies [52]. These differences between the crystal apatite morphology from Cu-doped glasses and those from undoped glasses could be explained by a possible incorporation of Cu into the apatite crystal lattice as have been reported previously [41], modifying both the lattice parameters and the crystal growth. For instance, if exist a substitution of Cu with Ca become important the difference in ionic radius (Cu^{+2} = 0.72 Å and Ca^{+2} = 0.99 Å) and charge [50, 53]. However, it seems that the incorporation of Cu into the HA structure depend on the characteristic of the glass as in Cu-doped borate glasses evidence of this incorporation was not found [50].

By incorporating Zn into both 58S and NaBG (figures 5(*c*) and (*d*), respectively) the formation of

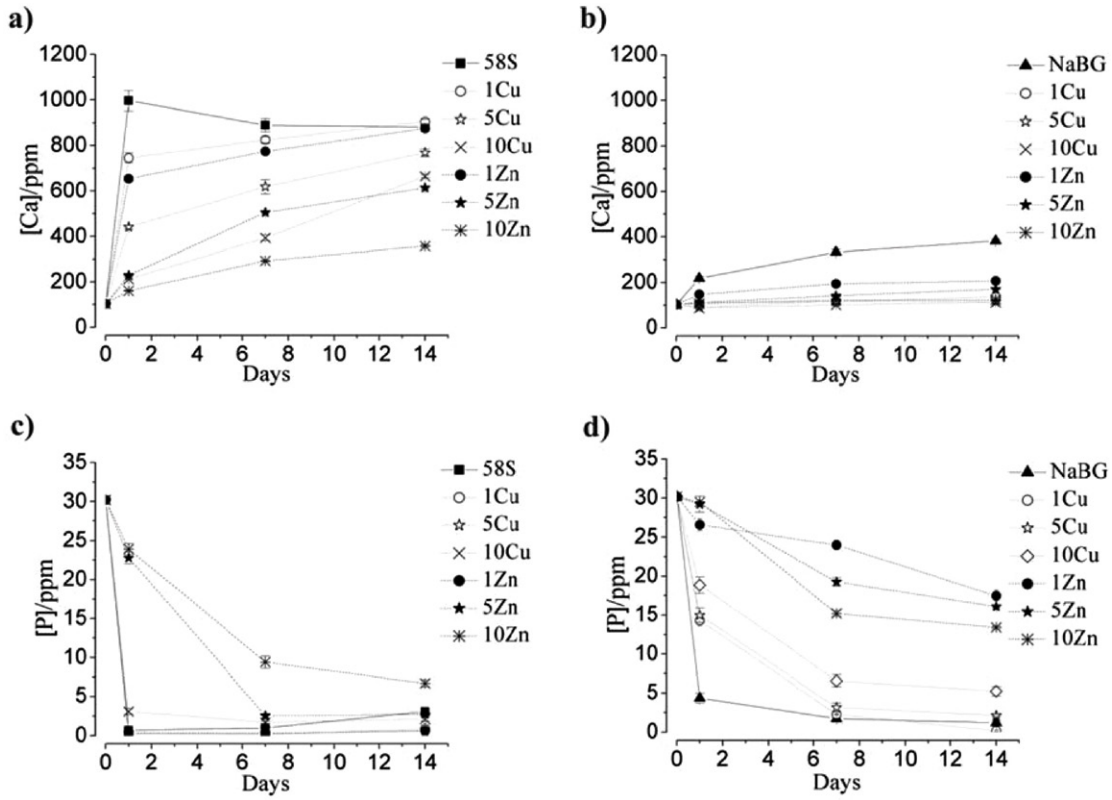

Figure 4. Changes of Ca and P concentrations during glass dissolution for 1, 7 and 14 d in SBF. (*a*) release of Ca from 58S derived glasses, (*b*) release of Ca from NaBG derived glasses, (*c*) adsorption of P from 58S derived glasses and (*d*) adsorption of P from NaBG derived glasses.

crystal apatites was also inhibited showing structures mainly amorphous during the different soaking times as reported previously [34, 54, 55]. Similar to the case of Cu-doped glasses, this inhibition can be also due to the substitution of Zn^{+2} for Ca^{+2} ions during apatite formation causing changes in the crystals by the difference in atomic radius (0.74 Å for Zn^{+2}) as it was demonstrated previously [56]. However, unlike glasses with copper, other effects caused by Zn such as structural stabilizing, as will be discussed later, can further cause the inhibition of the growth of apatite. The presence of 5 and 10 mol% of ZnO in NaBG promoted the formation of $CaSiO_2$ and cristobalite. SEM images from 1Zn–58S and 1Zn–NaBG at 7 d of immersion in SBF (figures 3(*e*) and (*f*)) did not show any evidence about the formation of apatite on the glass surfaces confirming the XRD results. Based on these results, we concluded that the *in vitro* bioactivity of glasses was less affected by Cu than by Zn. The effect of these metal ions on the bioactivity of the glasses was further confirmed by FTIR showing the same tendency that XRD results (data not shown).

The incorporation of Cu and Zn into 58S and NaBG glasses generated a lower amount of Ca released than undoped glasses with larger reductions coming from samples doped with Zn (figures 4(*a*) and (*b*)). In particular, the incorporation of these metals decreased the high release rate observed during the first day of soaking generating therefore a more controlled release. This controlled release of Ca^{+2} ions, especially at short times, can be related with the larger chemical stability and density of metal doped glass structure (higher network connectivity), thereby diminishing the dissolution and ion release [25, 51]. The metal based structural stabilization was also reflected in the adsorption of PO_4^{-3} in both doped matrices with NaBG-derived glasses having lower adsorption of PO_4^{-3} than 58S-derived glasses due to their lower surface area and higher crystallization. This chemical stability and low ion release of the glasses were larger in Zn-doped samples than in Cu-doped samples and it can be further related with the reduced apatite surface formation (NaBG based glasses) or its complete inhibition (58S based glasses) in Zn-doped glasses. These results can be explained considering the amphoteric characteristic of Zn^{+2} ions (4-fold and 6-fold coordination), which suggests that can have either tetrahedral coordination as the Si (network former) or octahedral coordination as a network modifier [40]. When Zn^{+2} ions participate as a network former, the polymerization degree or network connectivity associated with the formation of Zn–O–Zn and Si–O–Zn bonds is enhanced [51]. Have been showed that the geometries of the Zn tetrahedra present longer cation-oxygen distances and smaller angles with respect to the Si tetrahedra and to the interconnected Si-Zn tetrahedra, thereby reducing the volume between linked tetrahedral units producing a more dense and stable glass structure [36]. When Zn^{+2} ions otherwise act as network modifier replacing to Ca^{+2} ions the glass

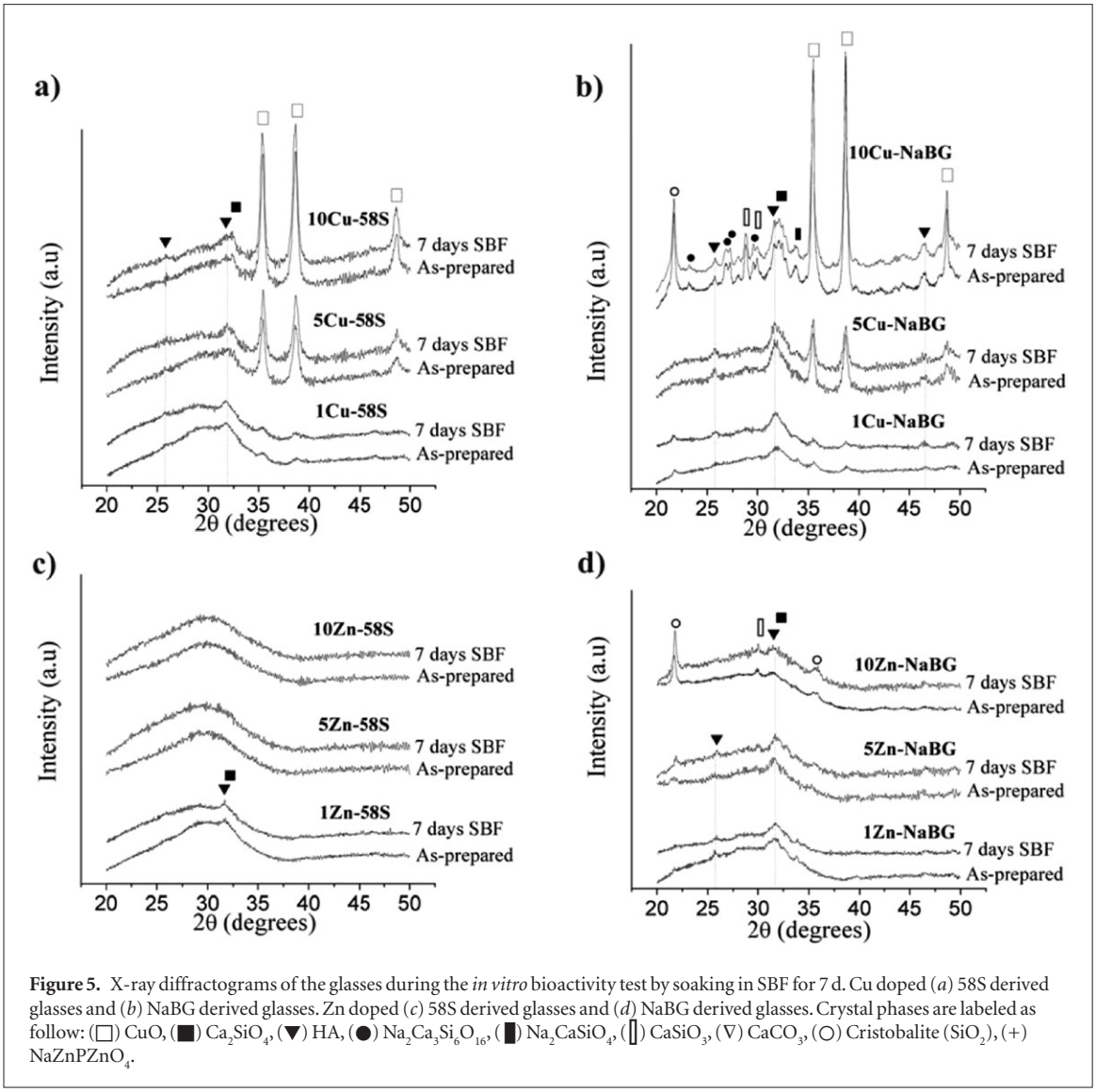

Figure 5. X-ray diffractograms of the glasses during the *in vitro* bioactivity test by soaking in SBF for 7 d. Cu doped (*a*) 58S derived glasses and (*b*) NaBG derived glasses. Zn doped (*c*) 58S derived glasses and (*d*) NaBG derived glasses. Crystal phases are labeled as follow: (□) CuO, (■) Ca_2SiO_4, (▼) HA, (●) $Na_2Ca_3Si_6O_{16}$, (▮) Na_2CaSiO_4, (▯) $CaSiO_3$, (∇) $CaCO_3$, (○) Cristobalite (SiO_2), (+) $NaZnPZnO_4$.

structure will also be strengthened since the ionic radii of Zn^{+2} are smaller than that of Ca^{+2} and Zn–O bonds are stronger than Na–O and Ca–O bonds, decreasing the ion release [51]. For the case of Cu^{+2} ions, these have an octahedral coordination and participate only as network modifier [41]. This behavior makes that Cu^{+2} ions have more mobility and generate glass structures less chemically stable and dense than that generated by Zn^{+2} ions.

3.3. *Releasing of Cu^{+2} and Zn^{+2} ions and pH changes in culture medium*

Figure 6 shows the release of Cu^{+2} and Zn^{+2} ions from the particles to the culture media (DMEM/F12) in order to related their release with the cytocompatibility to osteoblast SaOS-2. The release depended not only on the type of bioactive glass but also on the metal used as the amount of Cu^{+2} ions released was at least 10 times larger than Zn^{+2} ions for both glasses (58S and NaBG). The release of Cu^{+2} ions from 58S-derived glasses (figure 6(*a*)) was faster than NaBG-derived glasses (figure 6(*b*)) during the first day of soaking due to their high specific surface area and amorphicity allowing an increased dissolution. As time elapsed, the release rate of Cu^{+2} ions from 58S-derived glasses was decreased. The release of Cu^{+2} ions from NaBG-derived glasses (figure 6(*b*)) otherwise had a gradual increase up to 14 d.

The release of Zn^{+2} ions from 58S-derived glasses had a faster increase during the first day of soaking increasing the ion concentration in SBF although at longer times this was decreased (figure 6(*c*)). This decrease of the Zn^{+2} ion concentration in SBF after the first day of soaking was marked in 5Zn–58S and 10Zn–58S glasses while in 1Zn–58S the release of Zn^{+2} ions was almost zero during the whole soaking time. The formation of $Zn(OH)_2$ after the first day of soaking from dissolved Zn^{+2} ions in the media could explain this behaviour as previously reported [11]. The release of Zn^{+2} ions from NaBG-derived glasses (figure 6(*d*)) had a different kinetics (figure 6(*c*)). In sample with low amount of metal (1Zn–NaBG), an initial fast release followed by a stabilization at long times is observed meanwhile in samples with the highest amount of Zn (5Zn–NaBG and 10Zn–NaBG) a gradual release is displayed. The differences between the release of Cu^{+2} and Zn^{+2} ions from 58S and NaBG glasses could be due to differences in atomic radii and electronegativities of these

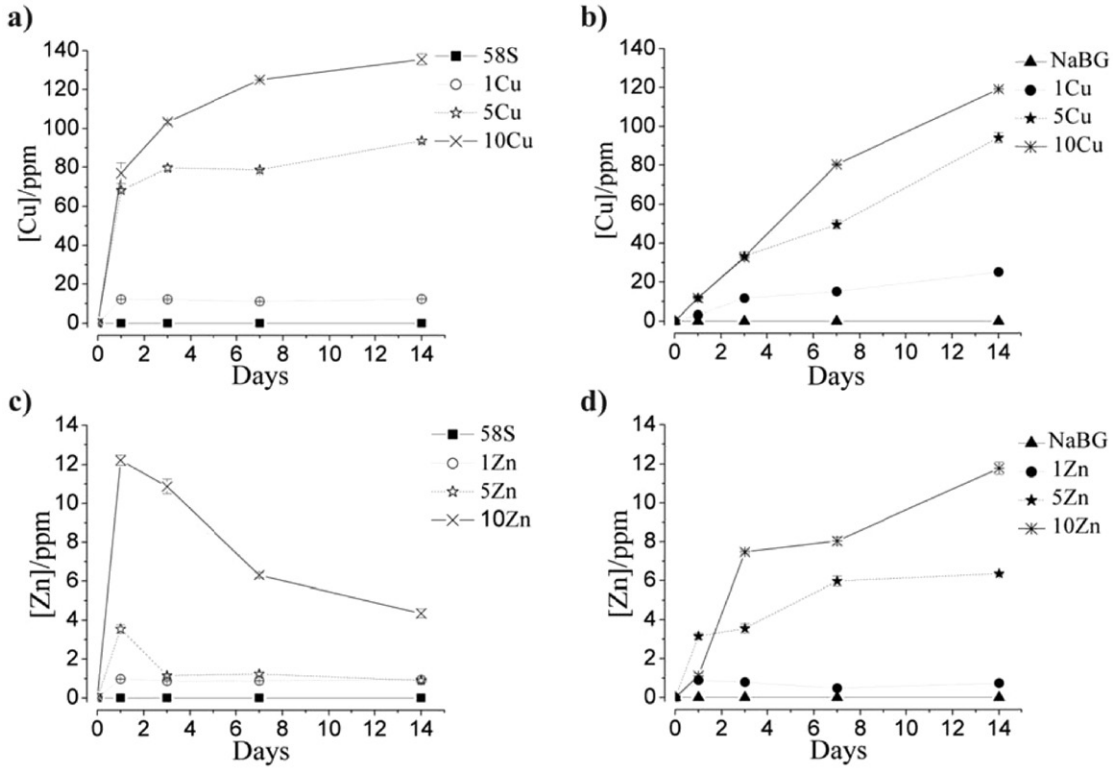

Figure 6. Release of Cu and Zn from bioactive glasses for 1, 3, 7 and 14 d. Cu release from (*a*) 58S derived glasses and (*b*) NaBG derived glasses. Zn release from (*c*) 58S derived glasses and (*d*) NaBG derived glasses.

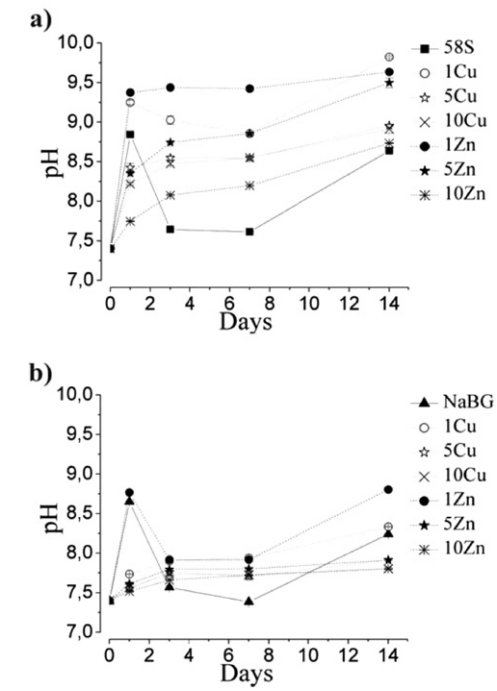

Figure 7. pH changes in DMEM/F12 by dissolution of the bioactive glasses. (*a*) 58S derived glasses and (*b*) NaBG derived glasses.

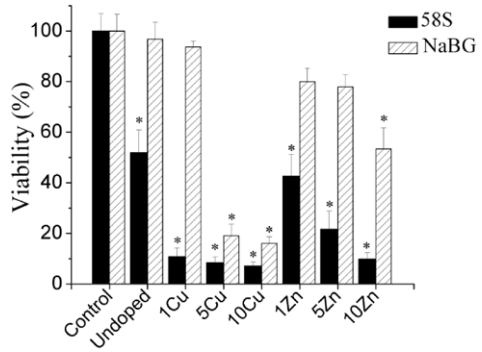

Figure 8. Cytocompatibility of undoped and Cu and Zn-doped glasses. *Statistically significant difference between experiment groups with control ($p < 0.01$).

metals generating different interactions with the non-bridging oxygen of the silicate tetrahedrons [11, 54]. For instance, as discussed above, Zn can strongly bind to the vitreous network forming tetrahedral structures as similar as Si, diminishing its release [35] whereas no evidence of Cu–O–Si bond formation and no connection of the Cu to the glass network has been found [57]. The weaker bond of Cu within of the glass structure might explain the higher release of Cu than Zn. Liu *et al* [50]. also found that the Cu^{+2} ion release was higher than that of Zn^{+2} ions for microfibers of the 13-93B3 borate glass co-doped with 0.4wt.% of CuO and 1wt.% of ZnO, which is consistent with our results.

The pH behavior is a relevant variable as cells are highly sensitive to changes in the physiological media (pH = 7.4). In general, bioactive glasses increase the pH of the medium by exchanging Ca^{+2} and Na^{+2} ions from the glass surface with H^{+} from the

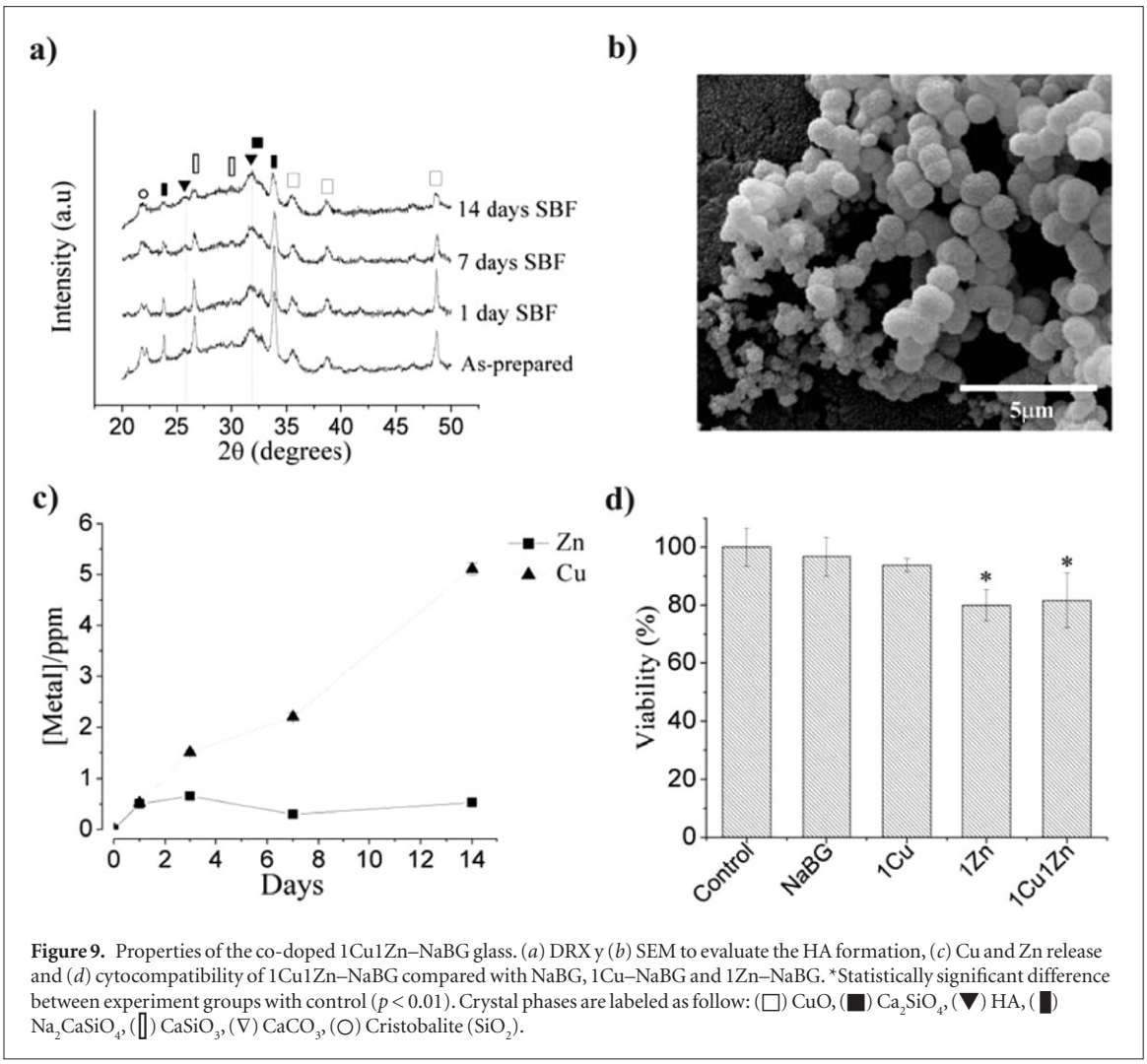

Figure 9. Properties of the co-doped 1Cu1Zn–NaBG glass. (*a*) DRX y (*b*) SEM to evaluate the HA formation, (*c*) Cu and Zn release and (*d*) cytocompatibility of 1Cu1Zn–NaBG compared with NaBG, 1Cu–NaBG and 1Zn–NaBG. *Statistically significant difference between experiment groups with control ($p < 0.01$). Crystal phases are labeled as follow: (□) CuO, (■) Ca_2SiO_4, (▼) HA, (▮) Na_2CaSiO_4, (▯) $CaSiO_3$, (∇) $CaCO_3$, (○) Cristobalite (SiO_2).

media [2]. According to figure 7, 58S glass generated a greater increase in pH than NaBG glass which can be explained by both the larger surface area and the lower crystallinity of 58S glass generating high ion release. These results showed that 58S-derived glasses could be more cytotoxic than NaBG-derived glasses because of the pH effect. 58S and NaBG glasses doped with low incorporation of Cu and Zn (1 mol% of CuO and ZnO) produced larger pH increase than undoped glasses. However, at higher metal incorporations (5 and 10 mol% of CuO or ZnO) the pH was lower than the undoped glasses. Both the lower amount of Ca in the doped glasses as replaced by the metal [25, 38] and the larger crystallization and network interconnectivity of the doped glasses, could explain the lower Ca^{+2} and Na^{+} ions release avoiding an increased pH. The changes in pH by doped glasses further depended on the type of metal incorporated as Zn-doped glasses produced lower pH values than Cu-doped glasses. This was due to the more stable glass structure generated by addition of Zn which diminished the Ca^{+2} and Na^{+} ions release.

3.4. Cytotoxicity test

The viability of SaOS-2 cells after exposure during 24 h to bioactive glasses is shown in figure 8. Undoped 58S glass was cytotoxic (viability around 50%) while NaBG glass did not show significant difference with control (viability around 95%). This confirms the strong effect of the higher release of cations (Ca^{+2}) from 58S glass generating a higher pH and therefore becoming toxic as previously reported for osteoblast (SaOS-2) and fibroblasts [34, 58]. Although, 58S glass is a well characterized materials, results about its cytotoxicity are contradictory as it depends on several parameters, such as: time of measurement, type of cells, concentration and pre-treatments of the glass, among others. For instance, Mortazavi *et al* [58] also reported toxicity to 24 and 48 h of contact between a ionic extract from 58S glass and the cells, but after 72 h the cell viability increased. Other studies have reported low or neither toxicity of the 58S glass, which can be explained by both the use of lower concentrations of glass or ionic extracts than our study (0.01 g ml^{-1}) [49], or the pre-treatment of the glass by immersion in culture medium previous to seed the cells, in order to avoid high ion release and pH increase during early times of culture [59]. The incorporation of either Cu or Zn to 58S glass generated even more cytotoxicity than undoped 58S glass with Cu^{+2} ions generating the highest toxicities reaching about 10% of cellular viability. The cytocompatibility of Cu and Zn-doped NaBG glasses otherwise depended on

both the type of metal ion and their incorporation. For instance, 1Cu–NaBG glass was not cytotoxic (around 94% of viability) while 5Cu–NaBG and 10Cu–NaBG glasses showed similar cytotoxicity (around 18% of viability for both glasses). The cytotoxicity of Zn-doped NaBG glasses also depended on the concentration of metal ion. 1Zn–NaBG and 5Zn–NaBG glasses were not cytotoxic meanwhile 10Zn–NaBG glass was cytotoxic decreasing the viability about 50%.

Previous results indicate that the toxicity in these systems relates with the metal ion concentration existing threshold as reported for Cu [11, 37, 60, 61] and Zn [10, 62–64] doped glasses. In our case, both Cu-doped (1Cu–58S, 5Cu–58S, 10Cu–58S, 5Cu–NaBG and 10Cu–NaBG) and Zn-doped (1Zn–58S, 5Zn–58S, 10Zn–58S and 10Zn–NaBG) glasses were cytotoxic releasing more than 11.7 and 3.5 ppm at 1 d, respectively. Samples 1Cu–NaBG, 1Zn–NaBG and 5Zn–NaBG were not cytotoxics releasing less than 3.0 ppm at 1 d. Based on these results a cytotoxicity threshold around 3.0 ppm for both metal ions can be stated. Above this threshold more than 30% of reduction in cell viability can be observed according to cytotoxicity criteria from standard ISO 10993:5 [29]. Because of the Zn^{+2} ions were released in much less amount than the Cu^{+2} ions from glasses a direct determination of the effect of the type of metal ion on the cytotoxicity for the same degree of incorporation, was not possible. However, the amount of Cu^{+2} ions released from 1Cu–NaBG glass was similar to the amount of Zn^{+2} ions released from the 5Zn–NaBG glass at 24 h (around 3.0 ppm) and both glasses were not cytotoxic. The cytotoxicity caused by the Cu^{+2} ions is related to the production of reactive oxygen species (Fenton type reaction) generating oxidative denaturation of proteins, peptides, DNA and phospholipids [11, 65]. In the case of Zn^{+2} ions, the mechanism is not yet clearly understood since its ion could not induces oxidative stress as it do not have a redox potential to generate radical species [64].

Because of 1Cu–NaBG and 1Zn–NaBG glasses were not cytotoxic, a glass co-doped with 1 mol% of CuO and 1 mol% of ZnO (1Cu1Zn–NaBG) was prepared seeking a potential therapeutic synergy between both ions. *In vitro* bioactivity, ions release and cytocompatibility were evaluated as shown in figure 9. The co-doped glass showed good bioactivity as the characteristic peaks of apatite layer after the first day of immersion in SBF appeared (figure 9(*a*)). This result was confirmed by the presence of apatite granules observed in SEM images (figure 9(*b*)). The release of Cu^{+2} and Zn^{+2} ions in the media (figure 9(*c*)) was given in a controlled manner with a low initial ion release and then a sustained release avoiding a possible toxic effect and also allowing a long-term duration of ion release. This was confirmed by the cytotoxicity test to osteoblasts after 24 h of contact (figure 9(*d*)) showing that 1Cu1Zn–NaBG glass present high cell viability for an ion release of 0.52 ppm of Cu^{+2} and 0.51 ppm of Zn^{+2}. This release values are lower than the cytotoxicity threshold (3.0 ppm) stated previously, validating this value. 1Cu1Zn–NaBG glass was therefore bioactive and no cytotoxic to SaOS-2 cells according to cytotoxicity criteria above described, allowing the conclusion that can be a potential therapeutic and anti-bacterial biomaterial due to the combination of the beneficial effects of Cu (angiogenic agent) and Zn (osteogenic agent). However, more studies are necessary to evaluate the biocompatibility of this glass for specific bone regeneration applications.

4. Conclusions

Ternary and quaternary sol–gel glasses doped with Cu and Zn were prepared and characterized allowing the conclusion that these metals can modulate the microstructure and textural properties of the glasses. Undoped 58S and NaBG glasses showed a surface hydroxyapatite layer after soaking in SBF reflecting their bioactivity and bone bonding ability. Metal ions inhibited the growth of apatite layers depending on the type of glass, the metal ion, and its concentration, with Zn-doped glasses showing the largest decreases especially at high concentration. The ion release and the pH change in the media also depended on the glass used with higher dissolutions observed in 58S than NaBG-derived glasses. By incorporating Cu^{+2} and Zn^{+2} ions, more stabilized glass structures were formed making more difficult the glass dissolution and the ion release, with Zn-doped glasses showing larger structural stabilization than Cu-doped glasses.

Pure 58S glass was cytotoxic to osteoblasts cells SaOS-2 (viability around 50%) while NaBG glass did not show significant difference with control (viability around 95%). In doped glasses, the toxicity was related with the metal ion concentration in the media with Zn-doped glasses having higher cellular viabilities than Cu-doped glasses. NaBG glasses doped with 1 mol% of CuO or ZnO and co-doped with 1 mol% of CuO and 1 mol% of ZnO (1Cu1Zn–NaBG) did not show cytotoxicity. 1Cu1Zn–NaBG glass was a bioactive and no cytotoxic glass, allowing the conclusion that can be a potential therapeutic and anti-bacterial biomaterial due to the combination of the beneficial effects of Cu (angiogenic agent) and Zn (osteogenic agent). However, more studies are necessary to evaluate the biocompatibility of this glass for specific bone regeneration applications.

Our results show that by changing the glass composition and by adding Cu or Zn, bioactive materials with different textures, bioactivity and cytocompatibility can be synthesized. These glasses therefore might be used in bone regeneration, for instance as a filler in polymer matrices with potential properties such as osteogenesis, angiogenesis and bacterial control.

Acknowledgments

We thank the Comisión Nacional de Investigación Científica y Tecnológica (CONICYT) for the PhD scholarship and financial support from Projects

Fondecyt No. and No. 1110078 and No. 1130241. We also want to thank to the Project Fondap CONICYT No 15090013 of the Centro de Excelencia en Geotermia de los Andes (CEGA) for supplying the SEM. Thanks to the Laboratory of Nanomaterials (Dr Cristian Covarrubias) for providing the FTIR and the Laboratory of biohydrometallurgy (Dr Tomas Vargas) for the measurements of metal ion concentration by AAS.

References

[1] Hench L L, Splinter R J, Allen W C and Greenlee T K 1971 Bonding mechanisms at the interface of ceramic prosthetic materials *J. Biomed. Mater. Res. Symp.* **5** 117–41
[2] Jones J R 2013 Review of bioactive glass: from Hench to hybrids *Acta Biomater.* **9** 4457–86
[3] Arcos D and Vallet-Regí M 2010 Sol–gel silica-based biomaterials and bone tissue regeneration *Acta Biomater.* **6** 2874–88
[4] Li R, Clark A E and Hench L L 1991 An investigation of bioactive glass powders by sol–gel processing *J. Appl. Biomater.* **2** 231–9
[5] Sepulveda P, Jones J R and Hench L L 2001 Characterization of melt-derived 45S5 and sol–gel—derived 58S bioactive glasses *J. Biomed. Mater. Res.* **58** 734–40
[6] Mouriño V, Cattalini J P and Boccaccini A R 2012 Metallic ions as therapeutic agents in tissue engineering scaffolds: an overview of their biological applications and strategies for new developments *J. R. Soc. Interface* **9** 401–19
[7] Hoppe A, Güldal N S and Boccaccini A R 2011 A review of the biological response to ionic dissolution products from bioactive glasses and glass-ceramics *Biomaterials* **32** 2757–74
[8] Hoppe A, Mouriño V and Boccaccini A R 2013 Therapeutic inorganic ions in bioactive glasses to enhance bone formation and beyond *Biomater. Sci.* **1** 254
[9] Habibovic P and Barralet J E 2011 Bioinorganics and biomaterials: bone repair *Acta Biomater.* **7** 3013–26
[10] Balamurugan A, Balossier G, Kannan S, Michel J, Rebelo A H S and Ferreira J M F 2007 Development and *in vitro* characterization of sol–gel derived CaO–P_2O_5–SiO_2–ZnO bioglass *Acta Biomater.* **3** 255–62
[11] Varmette E A, Nowalk J R, Flick L M and Hall M M 2009 Abrogation of the inflammatory response in LPS-stimulated RAW 264.7 murine macrophages by Zn- and Cu-doped bioactive sol–gel glasses *J. Biomed. Mater. Res.* Part A **90** 317–25
[12] Lakhkar N J, Lee I-H, Kim H-W, Salih V, Wall I B and Knowles J C 2012 Bone formation controlled by biologically relevant inorganic ions: role and controlled delivery from phosphate-based glasses *Adv. Drug Deliv. Rev.* **65** 405–20
[13] Nagata M and Lönnerdal B 2011 Role of zinc in cellular zinc trafficking and mineralization in a murine osteoblast-like cell line *J. Nutr. Biochem.* **22** 172–8
[14] Chen D, Waite L C and Pierce W M 1999 *In vitro* effects of zinc on markers of bone formation *Biol. Trace Elem. Res.* **68** 225–34
[15] Lusvardi G *et al* 2008 Properties of zinc releasing surfaces for clinical applications *J. Biomater. Appl.* **22** 505–26
[16] Oki A, Parveen B, Hossain S, Adeniji S and Donahue H 2004 Preparation and *in vitro* bioactivity of zinc containing sol–gel-derived bioglass materials *J. Biomed. Mater. Res.* A **69** 216–21
[17] Aina V, Malavasi G, Fiorio Pla A, Munaron L and Morterra C 2009 Zinc-containing bioactive glasses: surface reactivity and behaviour towards endothelial cells *Acta Biomater.* **5** 1211–22
[18] Haimi S *et al* 2009 Characterization of zinc-releasing 3D bioactive glass scaffolds and their effect on human adipose stem cell proliferation and osteogenic differentiation *Acta Biomater.* **5** 3122–31
[19] Srivastava A K and Pyare R 2012 Characterization of ZnO substituted 45S5 bioactive glasses and glass—ceramics *J. Mater. Sci. Res.* **1** 207–20
[20] Arredondo M and Núñez M T 2005 Iron and copper metabolism *Mol. Aspects Med.* **26** 313–27
[21] Finney L, Vogt S, Fukai T and Glesne D 2009 Copper and angiogenesis: unravelling a relationship key to cancer progression *Clin. Exp. Pharmacol. Physiol.* **36** 88–94
[22] Gérard C, Bordeleau L-J, Barralet J and Doillon C J 2010 The stimulation of angiogenesis and collagen deposition by copper *Biomaterials* **31** 824–31
[23] Hu G F 1998 Copper stimulates proliferation of human endothelial cells under culture *J. Cell. Biochem.* **69** 326–35
[24] Erol M, Özyu A, Mara M and Küçükbayrak S 2013 *In vitro* evaluation of Sr and Cu doped bioactive glasses *Adv. Sci. Lett.* **19** 3333–7
[25] Srivastava A K and Pyare R 2012 Characterization of CuO substituted 45S5 bioactive glasses and glass—ceramics *Int. J. Sci. Technol. Res.* **1** 28–41
[26] Palza H, Escobar B, Bejarano J, Bravo D, Diaz-Dosque M and Perez J 2013 Designing antimicrobial bioactive glass materials with embedded metal ions synthesized by the sol–gel method *Mater. Sci. Eng.* C **33** 3795–801
[27] Palza H, Gutiérrez S, Delgado K, Salazar O, Fuenzalida V, Avila J I, Figueroa G and Quijada R 2010 Toward tailor-made biocide materials based on poly(propylene)/copper nanoparticles *Macromol. Rapid Commun.* **31** 563–7
[28] Kokubo T and Takadama H 2006 How useful is SBF in predicting *in vivo* bone bioactivity? *Biomaterials* **27** 2907–15
[29] ISO/EN 10993-5 2009 *Biological Evaluation of Medical Devices, Part 5, Tests for Cytotoxicity: In Vitro Methods* vol 5 (Geneva: *International Organization for Standardization* (*ISO*))
[30] Labbaf S, Tsigkou O, Müller K H, Stevens M M, Porter A E and Jones J R 2011 Spherical bioactive glass particles and their interaction with human mesenchymal stem cells *in vitro* *Biomaterials* **32** 1010–8
[31] Siqueira R L, Peitl O and Zanotto E D 2011 Gel-derived SiO_2–CaO–Na_2O–P_2O_5 bioactive powders: synthesis and *in vitro* bioactivity *Mater. Sci. Eng.* C **31** 983–91
[32] Chen Q-Z, Li Y, Jin L-Y, Quinn J M W and Komesaroff P A 2010 A new sol–gel process for producing Na_2O-containing bioactive glass ceramics *Acta Biomater.* **6** 4143–53
[33] Lefebvre L, Chevalier J, Gremillard L, Zenati R, Thollet G, Bernache-Assolant D and Govin A 2007 Structural transformations of bioactive glass 45S5 with thermal treatments *Acta Mater.* **55** 3305–13
[34] Bini M, Grandi S, Capsoni D, Mustarelli P, Saino E and Visai L 2009 SiO_2–P_2O_5–CaO glasses and glass-ceramics with and without ZnO: relationships among composition, microstructure, and bioactivity *J. Phys. Chem.* C **113** 8821–8
[35] Aina V, Cerrato G, Martra G, Malavasi G, Lusvardi G and Menabue L 2013 Towards the controlled release of metal nanoparticles from biomaterials: physico-chemical, morphological and bioactivity features of Cu-containing sol–gel glasses *Appl. Surf. Sci.* **283** 240–8
[36] Lusvardi G, Malavasi G, Menabue L and Menziani M C 2002 Synthesis, characterization, and molecular dynamics simulation of Na_2O–CaO–SiO_2–ZnO glasses *J. Phys. Chem.* B **106** 9753–60
[37] Wu C, Zhou Y, Xu M, Han P, Chen L, Chang J and Xiao Y 2013 Copper-containing mesoporous bioactive glass scaffolds with multifunctional properties of angiogenesis capacity, osteostimulation and antibacterial activity *Biomaterials* **34** 422–33
[38] Goh Y-F, Alshemary A Z, Akram M, Abdul Kadir M R and Hussain R 2014 Bioactive glass: an *in-vitro* comparative study of doping with nanoscale copper and silver particles *Int. J. Appl. Glass Sci.* **5** 255–66
[39] Khalil E M A, ElBatal F H, Hamdy Y M, Zidan H M, Aziz M S and Abdelghany A M 2010 Infrared absorption spectra of transition metals-doped soda lime silica glasses *Physica* B **405** 1294–300
[40] Hudon P and Baker D R 2002 The nature of phase separation in binary oxide melts and glasses: I. Silicate systems *J. Non-Cryst. Solids* **303** 299–345

[41] Hoppe A et al 2013 In vitro reactivity of Cu doped 45S5 Bioglass® derived scaffolds for bone tissue engineering J. Mater. Chem. B 1 5659
[42] Sepulveda P, Jones J R and Hench L L 2002 In vitro dissolution of melt-derived 45S5 and sol–gel derived 58S bioactive glasses J. Biomed. Mater. Res. 61 301–11
[43] Goh Y-F, Alshemary A Z, Akram M, Abdul Kadir M R and Hussain R 2013 In vitro study of nano-sized zinc doped bioactive glass Mater. Chem. Phys. 137 1031–8
[44] Siqueira R L and Zanotto E D 2013 The influence of phosphorus precursors on the synthesis and bioactivity of SiO(2)-CaO-P (2)O (5) sol–gel glasses and glass-ceramics J. Mater. Sci. Mater. Med. 24 365–79
[45] Chen Q Z, Thompson I D and Boccaccini A R 2006 45S5 Bioglass-derived glass-ceramic scaffolds for bone tissue engineering Biomaterials 27 2414–25
[46] Wang P, Li C, Gong H, Jiang X, Wang H and Li K 2010 Effects of synthesis conditions on the morphology of hydroxyapatite nanoparticles produced by wet chemical process Powder Technol. 203 315–21
[47] Bi L, Jung S, Day D, Neidig K, Dusevich V, Eick D and Bonewald L 2012 Evaluation of bone regeneration, angiogenesis, and hydroxyapatite conversion in critical-sized rat calvarial defects implanted with bioactive glass scaffolds J. Biomed. Mater. Res. A 100 3267–75
[48] El-Kady A M and Ali A F 2012 Fabrication and characterization of ZnO modified bioactive glass nanoparticles Ceram. Int. 38 1195–204
[49] Bielby R C, Christodoulou I S, Pryce R S, Radford W J P, Hench L L and Polak J M 2004 Time- and concentration-dependent effects of dissolution products of 58S sol–gel bioactive glass on proliferation and differentiation of murine and human osteoblasts Tissue Eng. 10 1018–26
[50] Liu X, Rahaman M N and Day D E 2014 In vitro degradation and conversion of melt-derived microfibrous borate (13-93B3) bioactive glass doped with metal ions J. Am. Ceram. Soc. 97 3501–9
[51] Azevedo M M, Jell G, O'Donnell M D, Law R V., Hill R G and Stevens M M 2010 Synthesis and characterization of hypoxia-mimicking bioactive glasses for skeletal regeneration J. Mater. Chem. 20 8854
[52] Siqueira R L and Zanotto E D 2011 Facile route to obtain a highly bioactive SiO_2–CaO–Na_2O–P_2O_5 crystalline powder Mater. Sci. Eng. C 31 1791–9
[53] Liu G, Talley J W, Na C, Larson S L and Wolfe L G 2010 Copper doping improves hydroxyapatite sorption for arsenate in simulated groundwaters Environ. Sci. Technol. 44 1366–72
[54] Wers E, Bunetel L, Oudadesse H, Lefeuvre B, Lucas-Girot A, Mostafa A and Pellen P 2013 Effect of copper and zinc on the bioactivity and cells viability of bioactive glasses Bioceram. Dev. Appl. S1–013 doi:10.4172/2090-5025.S1-013
[55] Bigi A, Foresti E, Gandolfi M, Gazzano M, Roveri N, Gan M, Dipartimento N R and Bologna U 1995 Inhibiting effect of zinc on hydroxylapatite crystallization J. Inorg. Biochem. 58 49–58
[56] Ren F, Xin R, Ge X and Leng Y 2009 Characterization and structural analysis of zinc-substituted hydroxyapatites Acta Biomater. 5 3141–9
[57] Zhang Z, Dong H, Gorman B P, Mueller D W and Reidy R F 2004 Behavior of copper ions in silica xerogels J. Non-Cryst. Solids 341 157–61
[58] Mortazavi V, Nahrkhalaji M M, Fathi M H, Mousavi S B and Esfahani B N 2010 Antibacterial effects of sol–gel-derived bioactive glass nanoparticle on aerobic bacteria J. Biomed. Mater. Res. A 94 160–8
[59] Silver I A, Deas J and Erecin M 2001 Interactions of bioactive glasses with osteoblasts in vitro : effects of 45S5 Bioglass (R), and 58S and 77S bioactive glasses on metabolism, intracellular ion concentrations and cell viability Biomaterials 22 175–85
[60] Singh R P, Kumar S, Nada R and Prasad R 2006 Evaluation of copper toxicity in isolated human peripheral blood mononuclear cells and it's attenuation by zinc: ex vivo Mol. Cell. Biochem. 282 13–21
[61] Cao B, Zheng Y, Xi T, Zhang C, Song W, Burugapalli K, Yang H and Ma Y 2012 Concentration-dependent cytotoxicity of copper ions on mouse fibroblasts in vitro: effects of copper ion release from TCu380A versus TCu220C intra-uterine devices Biomed. Microdevices 14 709–20
[62] Lodemann U, Einspanier R, Scharfen F, Martens H and Bondzio A 2013 Effects of zinc on epithelial barrier properties and viability in a human and a porcine intestinal cell culture model Toxicol. In Vitro 27 834–43
[63] Zhang X Q, Yin L H, Tang M and Pu Y P 2011 ZnO, TiO_2, SiO_2, and Al_2O_3 nanoparticles-induced toxic effects on human fetal lung fibroblasts Biomed. Environ. Sci. 24 661–9
[64] Aina V, Perardi A, Bergandi L, Malavasi G, Menabue L, Morterra C and Ghigo D 2007 Cytotoxicity of zinc-containing bioactive glasses in contact with human osteoblasts Chem. Biol. Interact. 167 207–18
[65] Milkovic L, Hoppe A, Detsch R, Boccaccini A R and Zarkovic N 2014 Effects of Cu-doped 45S5 bioactive glass on the lipid peroxidation-associated growth of human osteoblast-like cells in vitro J. Biomed. Mater. Res. A 102 3556–61